STUDIA UBB CHEMIA, LXI, 3, Tom I, 2016 (p. 45-54)
(RECOMMENDED CITATION)

Dedicated to Professor Luminița Silaghi-Dumitrescu on the occasion of her 65th anniversary

COMPARATIVE COMPUTATIONAL CHARACTERIZATION OF FERRIC CYTOCHROME P450 AND SUPEROXIDE REDUCTASE BINDING TO CYANIDE

RADU SILAGHI-DUMITRESCU,[a*] DANIELA CIOLOBOC[a]

ABSTRACT. The active sites of the enzymes superoxide reductase (SOR) and cytochrome P450 feature square pyramidal FeN_4S centers, with a thiolate in axial position trans to the substrate binding site but with differing equatorial nitrogenous ligands. The respective catalytic cycles also share a common intermediate – a ferric-(hydro)peroxo species. The detailed catalytic mechanisms are still a matter of debate for both enzymes, as some of their key catalytic intermediates have very short lifetimes. Inhibitors such as cyanide were therefore often employed to probe active sites of these enzymes and identify important structural features controlling reactivity; among these studies, ENDOR spectral data on ferric-cyanide complexes were previously reported. Here, density functional calculations are employed in order to more accurately correlate the experimental data with electronic structure elements. The data are shown to be in good agreement with experiment and also provide new insight.

Keywords: *cytochrome P450, superoxide reductase, DFT, ENDOR*

INTRODUCTION

Superoxide reductases[1,2] and cytochromes P450[3] share a common motif at their active sites: a ferrous center with FeN_4S coordination, where a thiolate sulfur occupies an axial position, trans to the substrate binding site (cf. Figure 1). The four nitrogen atoms belong to a porphyrin in P450 and to four equatorial histidine side-chains in SOR.

[a] *Department of Chemistry, Babes-Bolyai University, 11 Arany Janos str, Cluj-Napoca, Romania*
** Corresponding author rsilaghi@chem.ubbcluj.ro*

Figure 1 illustrates the proposed catalytic cycles of SOR[4-11] and P450.[3] Two apparently orthogonal functions have been proposed for the thiolate ligand in P450 and SOR ferric-peroxo catalytic intermediates, under a framework known as “the push effect”[12]. Thus, at the ferric-hydroperoxo level, the thiolate is assumed to facilitate O-O bond cleavage in P450[3,13], while in SOR the same thiolate would favour Fe-O bond cleavage[14,15].

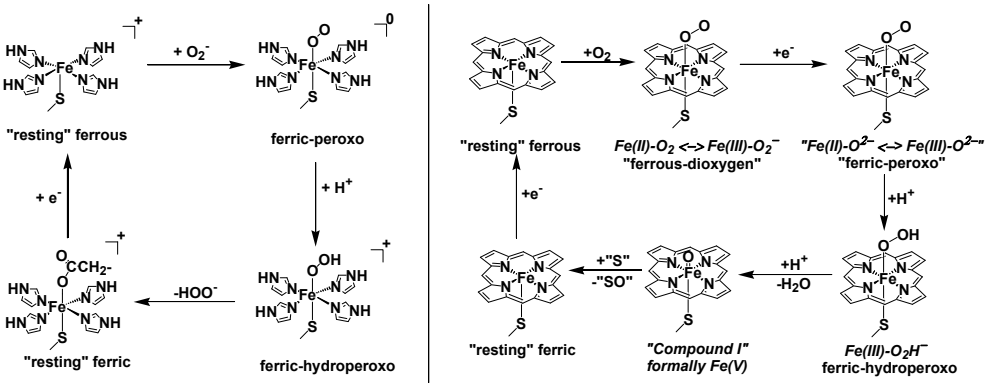

Figure 1. Proposed catalytic cycles of SOR (left) and P450 (right). For P450, “S” is a generic organic substrate that undergoes oxygen atom insertion to yield “SO”.

It was previously reported[9,10] that the trans (“push”) effect of the thiolate in heme-(hydro)peroxo adducts appears to be small at the geometric level. Thus, thiolate-ligated “ferric-peroxo” and ferric-hydroperoxo complexes featured Fe-O and O-O bond lengths very similar to those where the thiolate was replaced by imidazole, imidazolate, or phenoxide[9,10]. Slightly longer Fe-O *and* O-O bonds were noted in thiolate compared to non-thiolate models, possibly indicating an electronic basis for the proposed[14,15] apparently orthogonal facets of the “push effect”: Fe-O bond cleavage and O-O bond cleavage. On the other hand, the energetics of the “ferrous-dioxygen” - “ferric-peroxo” - ferric-hydroperoxo sequence were clearly different with thiolate compared to imidazole[9,10]. As expected based on simple charge arguments, the thiolate-ligated “ferric-peroxo” adduct had a much higher proton affinity than its imidazole-ligated counterpart. Along the same lines, reduction of “ferrous-dioxygen” to “ferric-peroxo” was harder to accomplish in thiolate models than in imidazole models[9,10]. The latter feature, which we described as “thiolate obstruction”, appears to also be active in nitric oxide reduction by another heme-thiolate active enzyme, P450nor, and its physiological utility as a “control switch” has been pointed out[9,10].

A comparison of SOR and P450 from the point of view of their cyanide adducts, employing ENDOR spectroscopy to probe spin density distribution within these two enzymes, has recently been reported, concluding strong similarities between SOR and P450[16,17]. While DFT calculations were employed in order to examine electronic structures[16,18], detailed calculations on ENDOR parameters have to our knowledge not been reported to date on the SOR and P450 cyanide adducts. Such data are reported here, further delineating differences between the two enzymes, and also addressing the issue of heterogeneity in cyanide binding geometry.

RESULTS AND DISCUSSION

DFT-optimized geometries (cf. Figure 2 and Table 1) are in good agreement with previous results on other low-spin Fe(III) adducts of SOR[18] and hemes[19-21]; for the latter, a general agreement with experiment was previously noted[21].

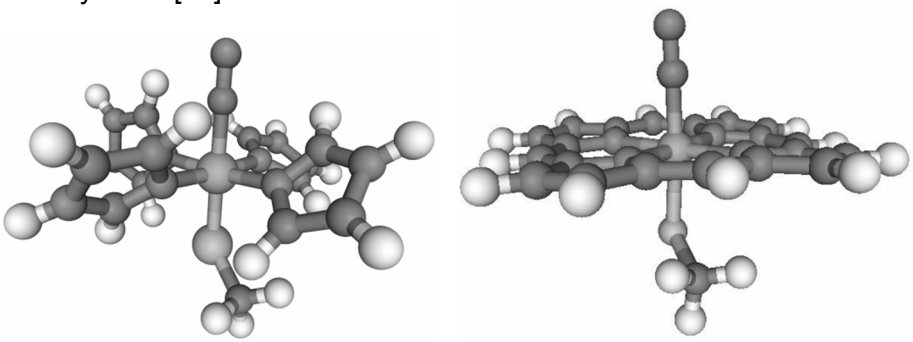

Figure 2. DFT-optimized S=1/2 Fe(III)-CN SOR and P450 models (following protocol described in [18,20,22]).

Essentially identical Fe-C-N moieties were obtained for models P450 (Figure 2), SOR (Figure 2), and for a truncated version of the Figure 2 SOR model, where the imidazole ligands were replaced with ammonia (SORr). SORr was further used in order to explore the conformational space. Despite previous proposals for a distinctly bent Fe-C-N unit in SOR, and despite the fact that the crystal structure of a P450 Fe(III)-cyanide adduct indeed shows a bent Fe-C-N moiety (pdb code 1N2N[23]), no local minimum for a bent Fe-C-N moiety could be located in any of the models examined here. When starting the geometry optimization from Fe-C-N angles ranging between 125º and 155º, the Fe-C-N moiety converged back to linearity.

However, modifying the Fe-C-N angle to 166º, 156º, 146º and 136º, with all other parameters unchanged, resulted in energy increases of 0.6, 1.9, 4.0, and 6.9 kcal/mol, respectively; a 5.5-kcal/mol energy difference was obtained after allowing the rest of the molecule to relax in response to the 136º-angle constraint. Also, it is unlikely that the bent local minima are actually differences in iron-imidazole(histidine) torsion angles. These very small energy differences suggest that within the respective protein active sites, factors as simple as even one strong hydrogen bond may in principle induce bending of the Fe-C-N moiety; steric constraints are also a likely cause of bending, at least in P450. Last but not least, it may be noted that the above-discussed data are an indication of a shallow potential surface around the Fe-C-N angle, and do not preclude the existence of local minima with a bent Fe-C-N moiety (or the identification thereof with a different functional or different numerical settings for convergence) – as long as any such minimum would be separated from the global minimum by extremely small barriers and would hence present negligible experimental relevance for the protein in its native environments.

The Fe-S bond in the SOR model is 0.1-0.2 Å shorter than measured by EXAFS for the resting ferrous and ferric states of SOR[24]. This difference is consistent with the high-spin character of the resting states compared to low-spin for the cyanide adducts. However, our previously calculated Fe-S bond length for the ferrous resting SOR was also 0.1-Å shorter than measured by EXAFS[18]. In principle, the SOR protein may impose an Fe-S bond longer than the intrinsic equilibrium distance, which, as shown by calculated Fe(III)-OO(H) distances[18] and as elaborated based on spectroscopy[24] and model compounds, would be beneficial (but not necessarily required[18]) for the SOR catalytic cycle. Tables 2 and 3 show that elongation of the Fe-S bond in the SOR Fe(III)-CN model by 0.2 Å (with a negligible energy cost, not shown), would affect $–SCH_3$ carbon and hydrogen spin densities and couplings to a small but detectable extent; the effect on the cyanide ligand appears to be very small but may in principle be detectable by virtue of a slightly altered isotropic coupling of the CN carbon atom (cf. Table 3).

Table 1. Key distances (Å) and angles for DFT-optimized SOR and P450 Fe(III)-CN models.

Model	Fe-S	Fe-CN	C-N	Fe-N[c]	Fe-C-N	S-Fe-C	H-C-S-Fe
SOR	2.24	1.94	1.18	2.04	179º	174º	-166º, 76º, -46º
SORr[a]	2.21	1.94	1.18	2.06	176º	177º	168º, 49º, -75º
SORrN[b]	2.14[b]	1.87	1.18	2.06	179º	179º	-
P450	2.28	1.96	1.18	2.01	179º	175º	174º

[a]equatorial imidazoles replaced with ammonia. [b]axial thiolate replaced with NH3; column 2 lists the axial Fe-NH_3 distance. [c]average of four equatorial Fe-N bonds.

Table 2. DFT-derived charges and spin densities (the latter are shown in parentheses).

Model	Fe	S	C^{methyl}	H^{methyl}	C^{CN}	N^{CN}
SOR	0.98 (0.77)	-0.21 (0.25)	-0.52 (-0.01)	0.18, 015, 0.19 (-0.000, 0.011, 0.008)	0.02 (-0.04)	-0.52 (0.05)
SORL[a]	0.99 (0.79)	-0.25 (0.23)	-0.52 (-0.01)	0.18, 015, 0.16 (-0.000, 0.010, 0.007)	0.03 (-0.04)	-0.52 (0.05)
SORr	0.83 (0.81)	-0.23 (0.21)	-0.53 (-0.01)	0.14, 0.21, 0.16 (-0.000, 0.010, 0.007)	-0.07 (-0.04)	-0.44 (0.06)
SORr bent	0.80 (0.82)	-0.22 (0.20)	-0.53 (-0.04)	0.14, 0.21, 0.17 (-0.001, 0.010, 0.006)	-0.13 (-0.04)	-0.35 (0.05)
P450	0.92 (0.87)	-0.18 (0.23)	-0.50 (-0.01)	0.1, 0.15, 0.15 (-0.001, 0.009, 0.008)	0.13 (-0.04)	-0.58 (0.05)
P450tw	0.92 (0.86)	-0.18 (0.24)	-0.50 (-0.01)	0.13, 0.11, 0.16 (0.011, 0.003, 0.002)	0.13 (-0.05)	-0.58 (0.04)

[a]Fe-S bond elongated by 0.2 Å compared to SOR while leaving all other geometrical parameters unchanged. The energy difference between SOR and SOR(long) was 2.8 kcal/mol.

For SOR, two of the methyl-thiolate protons are predicted to exhibit couplings that would make them readily detectable (cf. Table 3). These large couplings are due to isotropic components (15-26 MHz, cf. Table 3) and are one order of magnitude larger than those of other protons in the model (as exemplified by the third proton within the methyl-thiolate ligand). Correspondingly, the two strongly-coupled protons feature spin densities one order of magnitude higher than the third proton in the methyl-thiolate ligand (cf. Table 2). The origin of these increased spin densities is readily seen in hyperconjugation between the π electrons of the Fe-S bond and the C-H bonds of the Cysβ carbon. This hyperconjugation, although not explicitly discussed in each case, is indeed seen in all heme-thiolate and SOR adducts examined to date, including catalytically relevant ferrous-dioxygen, ferric(hydro)peroxo, Compound I, or Fe-NO adducts[5,18,20,21,25]. Because of the sterical steric constraints imposed by the imidazole ligand sitting above the Cys-β-carbon in SOR, rotation around the S-CH_3 bond in the SOR model (or in the actual protein) is impossible, and the S---CH hyperconjugation is maximized for the two protons placed ~symmetrically outside of the Fe-S-Cβ plane; the third proton (corresponding in fact to the Cys Cα carbon atom of SOR) is ~in the Fe-S-Cβ plane.

In the P450tw model, where the H-C-S-Fe dihedral was twisted to 25º compared to the value of ~0º in the global minimum, the isotropic Fermi contributions for the methyl protons, at 3 and 7 MHz respectively, are still distinctly above the values calculated for the other protons, and thus these protons might be observable by ENDOR. By contrast, in a P450 S=1/2

Fe(III)-OOH model with a similar H-C-S-Fe dihedral, the methyl protons have calculated Fermi contributions below 1 MHz, i.e., indistinguishable from other protons in the model and therefore unlikely to be observed experimentally by ENDOR[22].

Table3. Isotropic Fermi contact couplings (shown in italics) and anisotropic spin dipole couplings for SOR and P450 cyanide adduct models (in MHz for H and in Gauss for ^{13}C and ^{15}N).

Model	C^{methyl}	H^{methyl}	C^{CN}	N^{CN}
SOR	*-2.106* -0.282, 0.001, 0.282	*-0.437* -1.705, -1.435, 3.140 *26.723* 2.016, -1.357, 3.373 *16.692* -2.230, -1.178, 3.408	*-6.475* -1.065, -0.551, 1.616	*0.342* -0.670, -0.590, 1.259
SORL	*-1.664* -0.292, 0.003, 0.292	*-0.921* -1.540, -1.311, 2.851 *24.550* -1.895, -1.180, 3.075 *15.221* -2.098, -0.968, 3.067	*-6.891* -1.051, -0.525, 1.576	*0.367* -0.692, -0.590, 1.282
SORr	*-2.066* -0.243, 0.039, 0.204	*-0.730* -1.617, -1.352, 2.970 *13.372* -2.191, -1.260, 3.451 *23.109* -1.944, -1.426, 3.370	*-6.574* -1.184, -0.580, 1.763	*0.395* -0.804, -0.702, 1.506
SORr Bent	*-2.145* -0.229, 0.020, 0.209	*-0.939* -1.616, -1.313, 3.369 *12.623* -0.772, -0.445, 1.218 *22.422* -1.900, -1.469, 3.369	*-6.528* -1.242, -0.538, 1.781	*0.348* -0.918, -0.537, 1.455
P450 (global minimum)	*-2.038* -0.298, 0.071, 0.227	*-1.545* -1.602, -1.454, 3.056 *20.916* -2.300, -1.335, 3.635 *18.344* -2.483, -1.366, 3.848	-7.844 -1.007, -0.557, 1.564	0.332 -0.673, -0.550, 1.223
P450tw[a]	*-2.066* -0.277, 0.101, 0.176	*25.176*[b] -1.959, -1.607, 3.566 *7.642* -1.778, -1.515, 3.293 *3.752* -2.488, -1.522, 4.009	*-7.536* -0.997, -0.569, 1.566	*0.329* -0.647, -0.536, 1.183

[a]P450 model with H-C-S-Fe dihedral placed at 25º. [b]this proton does not exist in the actual P450 protein, where it it replaced by the cysteine Cα.

The isotropic Fermi contact couplings computed in Table 3 are in good agreement with experiment insofar as showing a detectable shift for the cyanide carbon atom, albeit smaller than measured experimentally (~7 MHz here, compared to 20-30 MHz in experiment)[16,17]. On the other hand, the anisotropic coupling constants range between 0.5 and 1.8, i.e. close to the experimental values[16,17]. However, our DFT-derived anisotropic constants appear to be affected to ~10% of their value when bending the Fe-C-N angle, whereas variations as high as 40% were proposed to arise from such bending, in order to interpret the fact that three different signals arising from iron-bound cyanide were observed experimentally by ENDOR[17].

Results obtained during molecular dynamics simulations illustrate the high mobility of the cyanide adduct. Figure 3 displays the evolution in time of the Fe-C-N angle over a course of 500 femtoseconds. The angle fluctuates very rapidly between the equilibrium point computed at 0 Kelvin (180^0) and the lowest value (158^0). These fluctuations may also engender fluctuations on electronic structure and, implicitly, modification of the anisotropic constants. On the other hand the high mobility of the cyanide adduct emphasizes the fact that multiple conformers are accessible which may impact on the ENDOR parameters; the frozen matrix and very low temperatures employed for these measurements may in principle help trap apparent local minima.

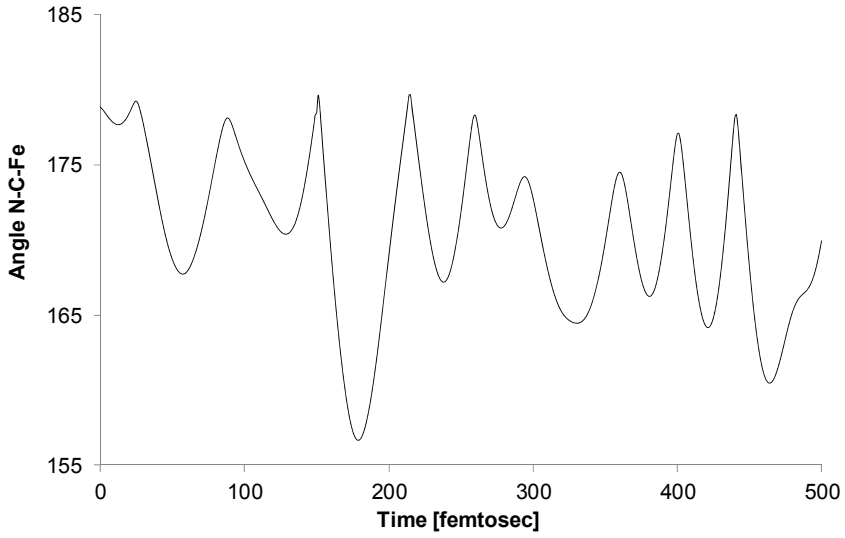

Figure 3. The Fe-C-N angle variation over a course of 500 femtoseconds.

The Fe-C bond length (data not shown) oscillates with an amplitude of 0.12 Å between 1.98 Å and 1.86 Å – a range also likely to have ENDOR-detectable effects on the electronic structures. Overall, this reveals that beyond the quasi-linear energy minimum of the ferric-cyanide adduct in SOR, the entire conformational space, with rotation around the Fe-C bond and bending of the Fe-C-N angle down to ~155º, is very much accessible, so that any influence from the second coordination sphere or beyond (e.g., the "distal" aminoacids E47 and K48, or indeed further from these) may easily lock the adduct into a distinct local minimum. The dynamics calculations also confirm a tendency of the Fe-C-N to gravitate around 170º, i.e. slightly but distinctly different from true linearity.

CONCLUSIONS

To conclude, computation of ENDOR-related parameters with DFT methods has allowed for a useful comparison between SOR and P450 active sites while also maintaining good agreement and even allowing for reinterpretation of some of the experimental data. The dynamics data reveal a relatively mobile Fe-C-N angle in SOR, with an average value distinctly below 180° in agreement with spectroscopic experimental data, even though the equilibrium geometry (and unique energy minimum) is precisely at 180°.

EXPERIMENTAL SECTION

Unless otherwise specified, geometries were optimized without any constraints with the BP86 functional, which uses the gradient-corrected exchange functional proposed by Becke (1988)[26], the correlation functional by Perdew (1986)[27], and the DN** numerical basis set (comparable in size to 6-31G**), as implemented in Spartan[28]. For the SCF calculations, a fine grid was used, and the convergence criteria were set to 10^{-6} (for the root-mean square of electron density) and 10^{-8} (energy), respectively. For geometry optimization, convergence criteria were set to 0.001 au (maximum gradient criterion) and 0.0003 (maximum displacement criterion). This methodology was previously shown to yield reasonable results on P450 and SOR models, as well as on related bioinorganic centers.[7,21,29-36] Hyperfine couplings, Mulliken charges and spin densities were obtained from UBP86/6-31G** energy calculations at geometries shown in Table 1, using the Gaussian98[37] software package. Molecular dynamics (MD) simulations were performed on the SOR model using the extended Lagrangian approach with the ADMP (Atom Centered Density Matrix Propagation) model using the Gaussian09 software package and the same functional and basis sets as for the energy profiles.

ACKNOWLEDGEMENTS

Funding from the Romanian Ministry for Education and Research (PCE 480/2012) is gratefully acknowledged. Prof. Donald M. Kurtz, Jr. (University of Texas at San Antonio) is thanked for helpful discussions.

REFERENCES

1. F.J. Jenney, M. Verhagen, X. Cui, M. Adams, *Science*, **1999**, *286*, 306-308
2. D.M.J. Kurtz, E. Coulter, *J. Biol. Inorg. Chem.*, **2002**, *6.*, 653-658.
3. M. Sono, M. P. Roach, E.D. Coulter, J.H. Dawson, *Chem. Rev.*, **1996**, *96*, 2841-2887.
4. E. Coulter, J. Emerson, D.J. Kurtz, D. Cabelli, *J. Am. Chem. Soc.*, **2000**, *122*, 11555-11556.
5. R. Silaghi-Dumitrescu, I. Silaghi-Dumitrescu, E.D. Coulter, J.P. Emerson, D.M. Kurtz, Jr., *J. Inorg. Biochem.*, **2001**, *86*, 432.
6. D.M. Kurtz, Jr., J.P. Emerson, R. Silaghi-Dumitrescu, I. Kung, A. Das, L. Ljungdahl, *J. Inorg. Biochem.*, **2003**, *96*, 69.
7. R. Silaghi-Dumitrescu, I. Silaghi-Dumitrescu, E. D. Coulter, D. M. Kurtz, Jr., *Inorg Chem*, **2003**, *42*, 446-56.
8. D.M. Kurtz, W.N. Lanzilotta, R. Silaghi-Dumitrescu, *Abstr. Pap. Amer. Chem. Soc*., **2004**, *227*, U1431-U1432.
9. R. Silaghi-Dumitrescu, *Rev. Roum. Chim*., **2008**, *53*, 1149-1156.
10. R. Silaghi-Dumitrescu, *Chem. Pap*., **2011**, *65*, 559-565.
11. A.A.A.A. Attia, D. Cioloboc, A. Lupan, R. Silaghi-Dumitrescu, *J. Biol. Inorg. Chem*., **2013**, *18*, 95-101.
12. J.H. Dawson, R.H. Holm, R.H. Trudell, G. Barth, R.E. Linder, E. Nunnernberg, C. Djerassi, S.C. Tang, *J. Am. Chem. Soc.*, **1976**, *98*, 3707.
13. F. Ogliaro, S. deVisser, S. Shaik, *J. Inorg. Biochem.*, **2002**, *91*, 554-567.
14. M.D. Clay, C.A. Cosper, F.E. Jenney, M.W. Adams, M.K. Johnson, *Proc. Natl. Acad. Sci. USA*, **2003**, *100*, 3796-3801.
15. J.A. Kovacs, *Chem. Rev.*, **2004**, 104, 825-848.
16. T.C. Yang, R.L. McNaughton, M.D. Clay, F.E. Jenney, Jr., R. Krishnan, D.M. Kurtz, Jr., M.W. Adams, M.K. Johnson, B.M. Hoffman, *J. Am. Chem. Soc.*, **2006**, *128*, 16566-78.
17. M.D. Clay, T.C. Yang, F.E. Jenney, Jr., I.Y. Kung, C.A. Cosper, R. Krishnan, D.M. Kurtz, Jr., M.W. Adams, B.M. Hoffman, M.K. Johnson, *Biochemistry*, **2006**, *45*, 427-38.
18. R. Silaghi-Dumitrescu, I. Silaghi-Dumitrescu, E.D. Coulter, D.M. Kurtz, Jr., *Inorg. Chem.*, **2003**, *42*, 446-456.
19. P. Rydberg, E. Sigfridsson, U. Ryde, *J. Biol. Inorg. Chem.*, **2004**, *9*, 203-223.

20. R. Silaghi-Dumitrescu, *J. Biol. Inorg. Chem.*, **2004**, *9*, 471-476.
21. R. Silaghi-Dumitrescu, I. Silaghi-Dumitrescu, *Rev. Roum. Chim.*, **2004**, *3-4*, 257-268.
22. R. Silaghi-Dumitrescu, C.E. Cooper, *Dalton Trans.*, **2005**, 3477-3482.
23. R. Fedorov, D.K. Ghosh, I. Schlichting, *Arch. Biochem. Biophys.*, **2003**, *409*, 25-31.
24. M.D. Clay, F.J. Jenney, P. Hagedoorn, G. George, M. Adams, M.K. Johnson, *J. Am. Chem. Soc.*, **2002**, *124*, 788-805.
25. R. Silaghi-Dumitrescu, *Eur. J. Inorg. Chem.*, **2003**, 1048-1052.
26. A.D. Becke, *Phys. Rev.*, **1988**, 3098-3100.
27. J.P. Perdew, *Phys. Rev.*, **1986**, *B33*, 8822-8824.
28. S. Spartan, *Spartan 5.0, Wavefunction, Inc., 18401 Von Karman Avenue Suite 370, Irvine, CA 92612 U.S.A.*
29. R. Silaghi-Dumitrescu, *Inorg. Chem.*, **2004**, *43*, 3715-3718.
30. R. Silaghi-Dumitrescu, *J. Biol. Inorg. Chem.*, **2004**, *9*, 471-476.
31. R. Silaghi-Dumitrescu, *Arch. Biochem. Biophys.*, **2004**, *424*, 137-140.
32. R. Silaghi-Dumitrescu, I. Silaghi-Dumitrescu, *J. Inorg. Biochem.*, **2006**, *100*, 161-6.
33. R. Silaghi-Dumitrescu, B.J. Reeder, P. Nicholls, C.E. Cooper, M.T. Wilson, *Biochem. J.*, **2007**, *403*, 391-395.
34. R. Silaghi-Dumitrescu, *Eur. J. Inorg. Chem.*, **2008**, 5404-5407.
35. A. Mot, Z. Kis, D.A. Svistunenko, G. Damian, R. Silaghi-Dumitrescu, S.V. Makarov, *Dalton Trans.*, **2010**, *39*, 1464-6.
36. R. Silaghi-Dumitrescu, S.V. Makarov, *Eur. J. Inorg. Chem.*, **2010**, 1129-1132.
37. *Gaussian 98 (Revision A.1), M.J. Frisch, G.W. Trucks, H.B. Schlegel, G.E. Scuseria, M.A. Robb, J.R. Cheeseman, V.G. Zakrzewski, J.A. Montgomery, R.E. Stratmann, J.C. Burant, S. Dapprich, J.M. Millam, A.D. Daniels, K.N. Kudin, M.C. Strain, O. Farkas, J. Tomasi, V. Barone, M. Cossi, R. Cammi, B. Mennucci, C. Pomelli, C. Adamo, S. Clifford, J. Ochterski, G.A. Petersson, P.Y. Ayala, Q. Cui, K. Morokuma, D.K. Malick, A.D. Rabuck, K. Raghavachari, J.B. Foresman, J. Cioslowski, J.V. Ortiz, B.B. Stefanov, G. Liu, A. Liashenko, P. Piskorz, I. Komaromi, R. Gomperts, R.L. Martin, D.J. Fox, T. Keith, M.A. Al-Laham, C.Y. Peng, A. Nanayakkara, C. Gonzalez, M. Challacombe, P.M.W. Gill, B.G. Johnson, W. Chen, M.W. Wong, J.L. Andres, M. Head-Gordon, E.S. Replogle and J.A. Pople, Gaussian, Inc., Pittsburgh PA, 1998.*